Mixing characteristics of different kneading elements: An experimental study

Nakayama, Yasuya
Department of Chemical Engineering, Kyushu University

Esaki, Satoshi
Department of Chemical Engineering, Kyushu University

Nakao, Kenta
Department of Chemical Engineering, Kyushu University

Kajiwara, Toshihisa
Department of Chemical Engineering, Kyushu University

他

出版情報：AIP conference proceedings. 2139 (1), pp.020005-, 2019-08-26. AIP Publishing
バージョン：
権利関係：

Mixing Characteristics of Different Kneading Elements: an Experimental Study

Yasuya Nakayama[a*], Satoshi Esaki[a], Kenta Nakao[a], Toshihisa Kajiwara[a], Takahide Takeuchi[b], Koichi Kimura[b], and Hideki. Tomiyama[b]

[a]*Department of Chemical Engineering, Kyushu University, 744 Motooka, Nishi-ku, Fukuoka 819-0395, Japan*
[b]*Hiroshima Plant, The Japan Steel Works Ltd. 1-6-1 Funakoshi-minami, Hiroshima 736-8602, Japan*

kajiwara@chem-eng.kyushu-u.ac.jp
nakayama@chem-eng.kyushu-u.ac.jp

Abstract. We discuss the melt-mixing characteristics of different geometries of pitched-tip kneading disks (ptKD). Extrusion experiment was performed under the fully-filled state in the kneading zone by controlling the fill lengths for different KDs. We study the variation of the particle size distribution and the rheological response of ABS (acrylonitrile-butadiene-styrene copolymer) caused by melt-mixing. We found that the increase or decrease of the fine and coarse particles depends on the type of KD. Furthermore, the change of the particle size distribution affects the storage modulus at low frequencies. From these results, different mixing characteristics of different KDs are evaluated.

Keywords: Twin-screw extrusion, Mixing element, ABS
PACS: 83.50.Xa Mixing and blending

INTRODUCTION

Mixing of highly viscous materials, such as polymer blends, polymer composites, and rubber compounds, is commonly performed in twin-screw devices, such as twin-screw extruders and twin-screw kneaders, because the material exchange between neighboring chambers is effective at mixing. The channel geometries in twin-screw devices, which is mainly determined by screw elements normally have the narrow gap regions, such as tip-barrel clearance and the intermeshing regions, which is mainly responsible for generating a high level of shear rate and shear stress. In contrast, the other regions from the narrow gaps are responsible for mixing, so that different designs of the mixing elements have been developed [1, 4, 5, 6, 7, 8]. Understanding the relation between the element geometries and the mixing characteristics is a key issue in optimizing the mixing process [1, 2, 3].

Mixture quality of a product is characterized in the two aspects that are the homogeneity in the spatial concentration distribution, and the size distribution of dispersed phases. The characteristics of a mixing process can be assessed through the mixture quality of the extrudate. Mixing process is mainly performed by the flow caused by rotation of the elements, and is most promoted when the material fully fills the melt-mixing zone. However, the channel inside a twin-screw extruder is not necessarily fully filled. Since degree of filling or fill length depends on the geometries of elements under a fixed throughput rate and screw rotation speed. When experimentally comparing the mixture characteristics for different elements under a fixed operation condition, difficulty comes from the difference of the fill lengths which directly affects the mixture quality of the extrudates. Intrinsic mixing characteristics of an element need to be measured at fully-filled state.

In this paper, we experimentally investigate the difference of the mixing characteristics of the pitched-tip kneading disks and the conventional one. Extrusion experiments with different elements under a fully-filled state in the melt-mixing zone and a given operation condition are performed. By analyzing the mixture quality of the extrudates, we discuss the mixing characteristics of the different elements.

EXPERIMENTAL

ABS (acrylonitrile butadiene styrene) resin (UMG-ABS: R-80) which contains 60 wt% polybutadiene rubber was diluted by adding SAN (styrene-acrylonitrile copolymer, UMG-ABS: S101N) resin to be 12 wt% of rubber. By this dilution, single rubber particles are easily identified from SEM image. Twin-screw extruder used in this study is TEX28V from Japan Steel Works Ltd. Melt-mixing zone was arranged to L/D=4.5 (equivalent to three segments of one piece in Fig. 2) just before the die (Fig. 1). Five different elements shown in Fig. 2 are tested for melt-mixing zone: one is conventional forward kneading disks (FKD), and the others are four different types of pitched-tip kneading disks (ptKD) which are denoted as Fs-Ft, Fs-Bt, Bs-Ft, and Bs-Bt where Fs/Bs indicates forward/backward disk stagger and Ft/Bt indicates the forward/backward pitched tips.

The difference in the pumping abilities of different elements results in difference in the fill length in the melt-mixing zone under a fixed throughput rate and screw rotation speed, leading to insufficient output of the intrinsic mixing characteristics which makes it difficult to compare different kneading elements. To overcome this difficulty, we explicitly set the melt-mixing zone to be fully-filled under a throughput rate and a screw rotation speed by adjusting the channel width in the die. The fully-filled state in the melt-mixing zone is monitored by the two pressure sensors equipped at the inlet of the melt-mixing zone. Pressure values as a function of the screw speed under 10 kg/h extrusion is shown in Fig. 3 where we can identify the fully-filled state at the change of the slope. Keeping the fully-filled state for different elements, ABS resin was melt-mixed under a throughput rate of 10kg/h and the screw rotation speed of 350 rpm with the barrel temperature of 200˚C. The size distribution of the rubber particle in the extrudates as well as the melt viscoelasticity are analyzed to discuss the mixing characteristics of the different elements.

Exrudates of ABS are compression molded into plates at a temperature above softening point. After that, ABS was stained with osmium tetraoxide to get a contrast between SAN matrix and polybutadiene rubber in SEM image. The preprocessed samples were observed by SEM (Zeiss ULTRA55, located at The Ultramicroscopy Research Center Kyushu University). Obtained SEM images were processed to be binarized using a software ImageJ to identify the single rubber particles (Fig. 4), from which the area-equivalent diameter is extracted to calculate the distribution of the rubber particle sizes.

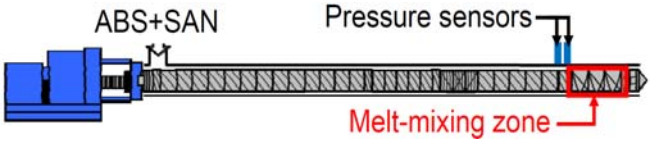

FIGURE 1. Configuration of the twin-screw extruder. Melt-mixing zone of L/D = 4.5 is set just before the die, at which different kneading elements are configured. Two pressure sensors are equipped adjacent to the inlet of the melt-mixing zone in order to detect the fully filled state of the melt-mixing zone.

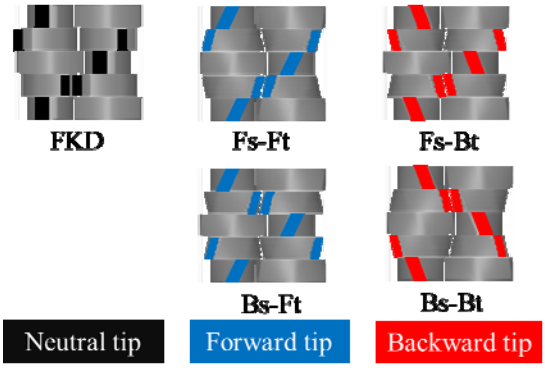

FIGURE 2. Top view of the five types of the kneading elements discussed in this paper. Each element has a dimension of L/D = 1.5.

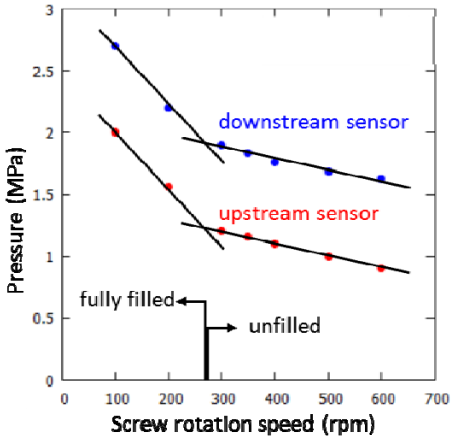

FIGURE 3. Pressure values from the two sensors at the inlet of the melt-mixing zone as a function of screw rotation speed under a constant throughput of 10 kg/h.

The particle size in the polymer composites is known to affect the modulus amplitude as well as the long-time response [9, 10, 11]. By analyzing the melt viscoelasticity of the extrudates, the mixing characteristics of different elements can be evaluated. The dynamic shear moduli of the molten extrudates were measured at different temperatures under a nitrogen atmosphere using a rheometer (Rheosol-G1000, UBM, Kyoto, Japan) in parallel-plate geometry with a plate diameter of 25 mm. The strain amplitude was set at 0.1, which falls within the linear response regime.

RESULTS AND DISCUSSION

Figure 4 shows the binarized SEM images of the extrudates with different elements as well as that of the unprocessed sample for comparison. In all the cases in Fig. 4, the particles of polybutadiene rubber (black) are almost evenly distributed in the matrix of SAN (white), and no significant aggregation is observed. The mean diameter of the particles in the unprocessed sample is 259 nm consistent with the value reported by the supplier, while those after melt-mixing lie between 259 and 277 nm. The average size of the rubber phase rarely changes by melt-mixing since the mean size in the original ABS is already small. In contrast, distribution in particle size is observed in Fig. 4 and varies between the melt-mixing elements.

Fig. 5 shows the probability density functions of particle diameter in the extrudates, and clearly demonstrates that the change in the particle size distribution depends on the melt-mixing elements. For the unprocessed sample, two peaks at around 200 nm and 120 nm, which are less than the mean value, are observed. For further quantification of the change in particle size distribution, we divide the size domain into four intervals with three quartile points in the distribution of the unprocessed sample, and calculate the relative change in the fractions of the four intervals.

Figure 6 shows the relative changes in the fractions of the four intervals from those of the unprocessed sample. For Fs-Ft and Fs-Bt, the change in the size distribution is relatively small (Figs. 5(a) and 6), but we observe the decrease in the fractions of fine particles smaller than 206.8 nm and the increase in the fractions of coarse particles. For Bs-Bt, the increase in the coarsest-particle fraction (larger than 331.7 nm) is the highest. In contrast, for FKD and Bs-Ft, the increase in the fine-particle fraction (smaller than 149.7 nm) is noticeable (see also Fig. 5(b)). Especially for Bs-Ft, only the finest-particle fraction (smaller than 149.7 nm) increases, and the other three fractions of the particle decrease, showing a remarkable size reduction with Bs-Ft.

The increase of the first fraction (smaller than 149.7 nm) reflects a dispersive ability. The results in Fig. 6 suggest a certain level of dispersive ability of FKD and Bs-Ft. On the other hand, the increase of the

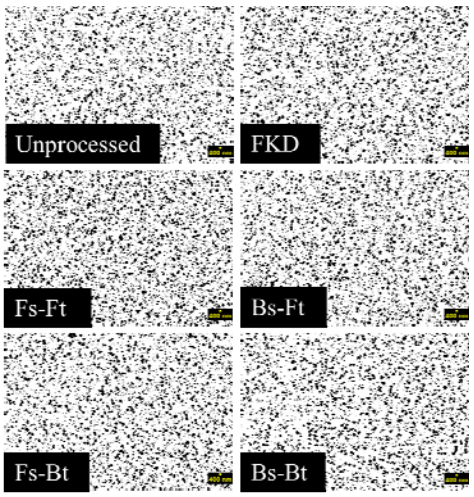

FIGURE 4. Binarized SEM images of the extrudates melt-mixed with different kneading elements. Black region is the rubber particles of polybutadiene while the white region is styrene-acrylonitrile copolymer which consists of the matrix of ABS resin.

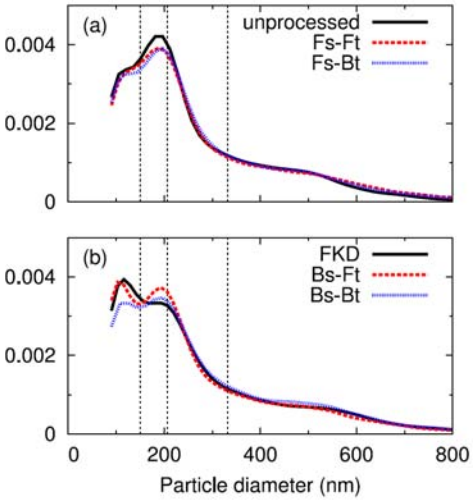

FIGURE 5. Probability density function of particle diameter for the extrudates melt-mixed with different kneading elements. The vertical dotted lines indicate the quartiles in the distribution of the unprocessed sample.

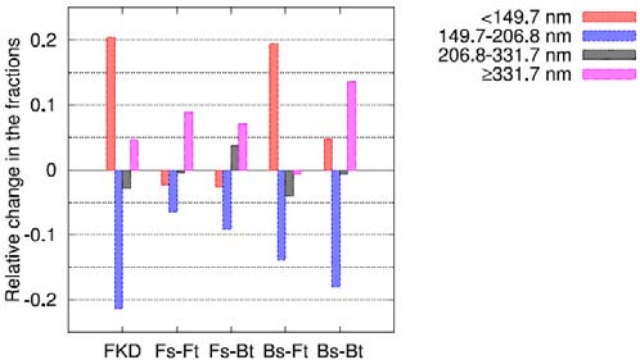

FIGURE 6. Relative changes in the fractions in the four intervals, which is defined by the quartiles of the unprocessed sample shown in Fig. 5, after melt-mixing with the different kneading elements.

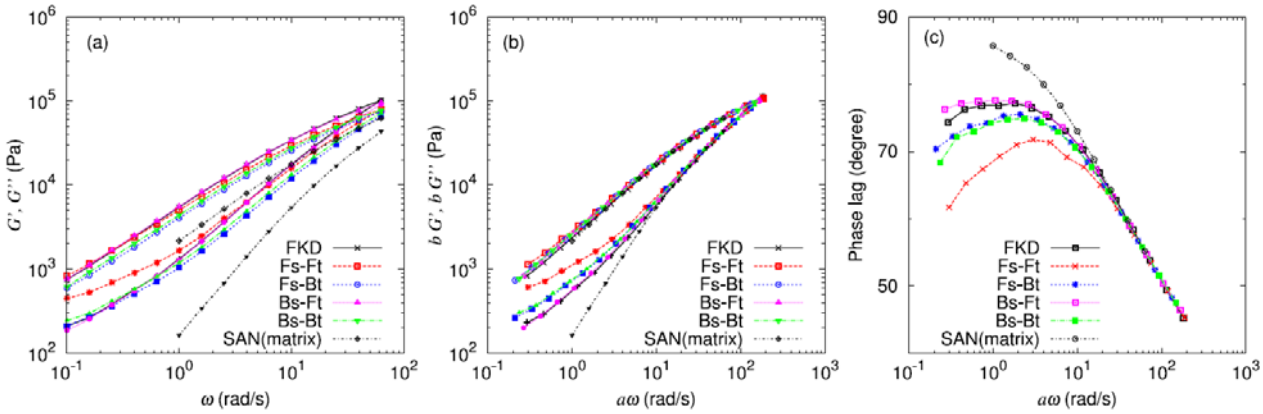

FIGURE 7. Linear modulus of the extrudates melt-mixed by different kneading elements: (a) raw data at 200◦C, (b) the data shifted to that of SAN, and (c) the phase lag after the frequency shift to SAN data.

fourth fraction (larger than 331.7 nm) reflects a degree of weakness of mixing, supposing that the aggregation of fine particles induces the coarsening of particles due to weak mixing. The results in Fig. 6 suggest a high mixing ability of Bs-Ft as well as a modest mixing ability of Fs-Ft, Fs-Bt, and Bs-Bt. From the change in the size distribution, the difference of dispersive and mixing abilities for different kneading elements were characterized.

The change in the particle size distribution caused by the melt-mixing modifies the rheological response of the extrudates. Fig. 7(a) shows the storage and loss moduli at 200°C of the extrudates by the different kneading elements as well as those of SAN, the matrix of the ABS, for comparison. At high frequencies, we observe that the modulus has a similar frequency-dependence as for SAN, but the amplitude of the modulus depends on the kneading elements. Furthermore, at low frequencies where the terminal region for SAN, the storage modulus, G', for the extrudates starts to increase. Prior works reported, as the rubber content increases, a plateau of G' develops at low frequencies, which is called the second plateau [9, 10, 11]. Since the rubber content of 20 wt% used in this repor is relatively low, only the onset of the second plateau was observed.

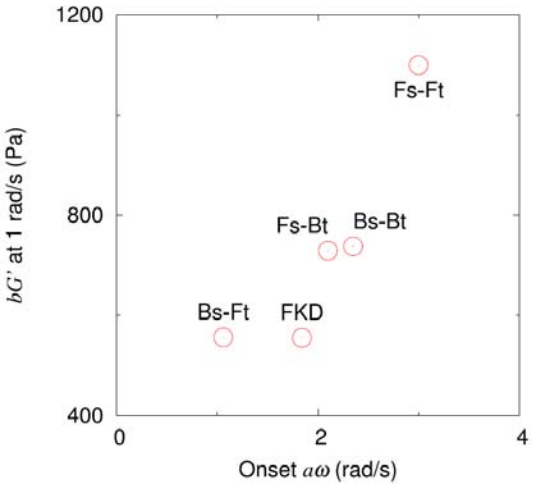

FIGURE 8. Storage modulus at 1 rad/s from the low-frequency elastic regime and onset frequency of the second plateau, at which frequency the phase lag have a maximum.

In Fig. 7(b), $G'(\omega)$ and $G''(\omega)$ for the extrudates are shifted to those for SAN, showing that the loss modulus $bG''(a\omega)$ almost coincides irrespective of the mixing elements, but the onset of the second plateau in the storage modulus $bG'(a\omega)$ depends on the mixing elements. Fig. 7(c) shows the phase lag, G''/G', after shifting to that for SAN, from which we observe that maxima in the phase lag clearly indicate the onset of the second plateau.

In Fig. 8, we plot the onset frequency of the second plateau determined from Fig. 7(c) and bG' value at 1 rad/s from Fig. 7(b) as a measure for the second plateau. Fig. 8 demonstrates a correlation between a value of bG' at a low frequency and the onset frequency, indicating that the onset frequency can characterize the low-frequency elastic property of ABS resin. Moreover, the shift factor for the amplitude of modulus, b, for high frequencies has a correlation with the onset frequency (Figure not shown). From these results, the effects of the size distribution induced by the melt-mixing are supposed to be reflected primarily in the onset frequency of the second plateau.

The onset frequency of the second plateau is low for Bs-Ft and FKD, for which cases the increase in the fine-particle fraction in the extrudates is a high level. The onset frequency is high for other cases where the coarse-particle fraction increases. Although the onset frequency itself describes only a limited aspect of the quality of the extrudates in comparison with the size distribution, but it surely shows some dependence on the size distribution.

CONCLUSIONS

Mixing characteristics of four kinds of pitched-tip kneading disks and a conventional kneading disk were analyzed experimentally. In order to evaluate intrinsic mixing characteristics of the kneading elements with different pumping abilities, we maintained the melt-mixing zone to be fully filled under a given throughput rate and a screw rotation speed by adjusting the pressure at the downstream of the melt-mixing zone. The melt-mixing of an ABS resin resulted in the change in the distribution of the rubber particle size. The particle size distributions of the extrudates with different elements reflect the mixing characteristics of the elements. It turns out that Bs-Ft ptKD and a conventional FKD have a high level of dispersive ability while Fs-Ft and Bs-Bt ptKDs have a suppressed mixing ability, and Fs-Bt ptKD have a moderate level of mixing. Furthermore, the changes in the particle size distributions were reflected in the melt rheology of the extrudates. Figure 9 shows the relative changes in the fractions of the intervals of the finest and coarsest particles, qualitatively indicating different mixing characteristics of the different elements.

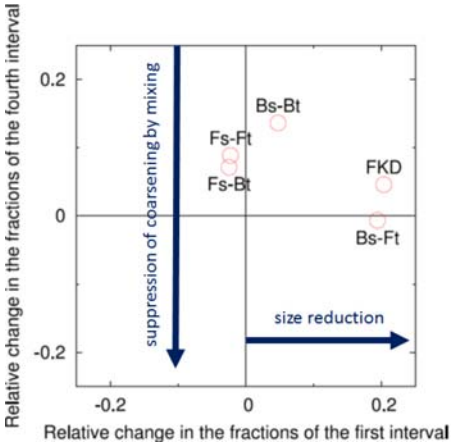

FIGURE 9. Relative changes in the fractions of the first (finest particles) and fourth (coarsest particles) intervals of the particle size distributions. The increase in the fine-particle fraction reflects the dispersive ability while the decrease in the coarse-particle fraction reflects the mixing ability.

ACKNOWLEDGMENTS

This work has been supported by Grants-in-Aid for Scientific Research (JSPS KAKENHI) under Grants Nos. 26400433, and 15H04175. Financial support from Hosokawa Powder Technology Foundation is also greatfully acknowledged. The numerical calculations were partly carried out using the computer facilities at the Research Institute for Information Technology at Kyushu University. The SEM observation was carried out at the Ultramicroscopy Research Center, Kyushu University.

REFERENCES

1. K. Kohlgruber, *Co-Rotating Twin Screw Extruder*, Munich, Hanser, 2007.
2. C. Rauwendaal, *Polymer Extrusion, 5 ed.*, Munich, Hanser, Munich, 2014.
3. Y. Nakayama, T. Kajiwara, and T. Masaki, *AIChE J.* **62**, 2563 (2016).
4. Y. Nakayama *et al.*, *Chem. Eng. Sci.* **66**, 103 (2011).
5. Y. Nakayama *et al.*, *Nihon Reoroji Gakkaishi (J. Soc. Rheol. Jpn.)*, **44**, 281 (2016).
6. K. Hirata *et al.*, *Intern. Polym. Process.*, **28**, 368 (2013).
7. K. Hirata *et al.*, *Polym. Eng. Sci.*, **54**, 2005 (2014).
8. S. Yamada *et al.*, *Intern. Polym. Process.*, **30**, 451 (2015).
9. Y. Aoki, *J. Soc. Rheol. Jpn.*, **7**, 20 (1979).
10. L. Castellani and P. Lomellini, *Rheol. Acta*, **33**, 446 (1994).
11. J. J. Cai and R. Salovey, *Polym. Eng. Sci.*, **39**, 1696 (1999).